Science Immunology
AAAS

immunology.sciencemag.org/cgi/content/full/3/27/eaas9822/DC1

Supplementary Materials for

Clonal expansion of vaccine-elicited T cells is independent of aerobic glycolysis

Jared Klarquist, Alisha Chitrakar, Nathan D. Pennock, Augustus M. Kilgore, Trevor Blain, Connie Zheng, Thomas Danhorn, Kendra Walton, Li Jiang, Jie Sun, Christopher A. Hunter, Angelo D'Alessandro, Ross M. Kedl*

*Corresponding author. Email: ross.kedl@ucdenver.edu

Published 7 September 2018, *Sci. Immunol.* **3**, eaas9822 (2018)
DOI: 10.1126/sciimmunol.aas9822

The PDF file includes:

Other Supplementary Material for this manuscript includes the following:

(available at immunology.sciencemag.org/cgi/content/full/3/27/eaas9822/DC1)

Supplementary methods:

Flow Cytometric Analyses

Spleens were harvested seven d.p.i. for flow cytometric analysis, five d.p.i. for metabolic flux assays, or three d.p.i. for flow cytometric analysis of transcription factors. For day 3 time points, tetramer staining cells were enriched using magnetic columns as previously described (*66*). After red blood cell lysis, viable lymphocytes were counted using a Vi-Cell automated cell counter (Beckman Coulter). Cells were then incubated with αCD16/32 (clone 2.4G2; hybridoma supernatant) and tetramer stained as previously described (*24*), or in the case of OT-1 transfer, cells were stained for CD45.1 (clone A20; BioLegend). K^b-SIINFEKL, K^b-B8R, D^b-PA224, and D^b-NP396 tetramers were provided by the NIH Tetramer Core. Cell surface antibodies included B220 (RA3-6B2), CD8a (53-6.7), CD3e (145-2C11), CD44 (IM7), CD62L (MEL-14), CD122 (TM-β1), CD127 (A7R34; Tonbo), CXCR3 (CXCR3-173), Glut-1 (202915; R&D Systems) and KLRG1 (2F1/KLRG1) (all from BioLegend, unless otherwise noted). For glucose uptake experiments, cells were incubated with 100uM 2-NBDG (Sigma) in PBS for 15 minutes at 37C. For transcription factor analysis, cells were surface stained in PBS containing 2% FBS, then fixed and permeabilized using eBioscience Foxp3 fixation/permeabilization buffers (ThermoFisher) and stained for Tbet (4B10, BioLegend), Eomes (Dan11mag, eBioscience), IRF4 (3E4, eBioscience), pAKT (D9E), mTOR (S2481), cMyc (D84C12), p70pS6K (S371), and p4EBP1 (T37/46; 236B4) (all from Cell Signaling Technology, unless otherwise noted). Intracellular cytokine staining was performed in the same manner as transcription factors after a 5 hour incubation at 37C with 2 μg/ml SIINFEKL peptide. $CD8^+$ T cells were stained for intracellular IFNγ (XMG1.2), TNFα (MP6-XT22), and IL-2 (JES6-5H4); granzyme B (GB11; all from BioLegend) was stained directly *ex vivo* and analyzed on tetramer-positive cells. Flow cytometry data were acquired on a four laser (405, 488, 561, 638 nm) CytoFLEX S flow cytometer (Beckman Coulter) and analysis was performed using FlowJo (versions 9.9.4 and 10.4; BD Biosciences).

OT-1 Isolation and Transfer

WT and IL-27R$\alpha^{-/-}$ CD45.1+ OT-1 cells were enriched from unchallenged mouse spleens by negative magnetic separation according to the manufacturer's protocol (BioLegend). Purified OT-1 T cells were transferred one day prior to infectious challenge or immunization by tail vein injection at 5×10^3 per mouse per genotype for co-transfer transcription factor analyses, or 5×10^4 cells per mouse for metabolic flux assays, in 200ul PBS. Spleen single-cell suspensions were enriched for CD8+ T cells 1-3 d.p.i. for transcription factor analyses, or 5 d.p.i. by staining with biotinylated αCD4, αCD19, and αTer119 antibodies (GK1.5, 1D3, and TER-119; BioLegend and Tonbo), followed by streptavidin-labelled nanobeads (BioLegend), and selection over magnetic columns (Miltenyi). For metabolic flux assays, cells were further purified via positive selection by staining with αCD45.1-APC (A20; BioLegend) and αAPC-labelled nanobeads (BioLegend). For RNA sequencing, microarray analysis, proteomics, and transmission electron microscopy, OT1s were then further purified using a FACSAria Fusion (BD Biosciences) cell sorter.

Metabolic Flux Assays

Extracellular acidification rates (ECAR) and oxygen consumption rates (OCR) were determined using Seahorse XF24 and XFe96 Analyzers (Agilent). Purified OT-1 T cells were seeded on poly-D-lysine (Sigma)-coated 24-well or 96-well plates (Agilent) at 10^6 cells per well, or $1.5\text{-}2 \times 10^5$ cells per well, respectively, in Seahorse XF RPMI media containing 2 mM L-glutamine with (OCR measurements) or without (ECAR measurements) 10 mM D-glucose. Plates were degassed for 1 hour at 37°C without CO_2 prior to ECAR and OCR measurements. ECAR was measured before and after injecting: basal media, 10mM D-glucose, 1 uM oligomycin, and 50 mM 2-deoxy-D-glucose (2-DG). OCR was measured before and after injecting: 1 uM oligomycin, 1 uM carbonyl cyanide 4-(trifluoromethoxy) phenylhydrazone (FCCP), 4 uM Antimycin A and 1 uM rotenone. Injected compound (Sigma) concentrations are listed as final concentrations after injection. Aerobic glycolysis was determined by subtracting average ECAR

values after 2-DG administration from average basal ECAR values. Glycolytic capacity was defined as the average ECAR values after oligomycin administration minus the average ECAR values after 2-DG administration. Baseline ATP production was determined by subtracting the average OCR values obtained after oligomycin administration from the average basal OCR values. Spare respiratory capacity was defined as the average OCR values after FCCP administration minus the average baseline OCR values.

RNA sequencing, Microarray, and Proteomics Analyses

Affymetrix Gene Array: OVA- specific $CD8^+$ T cells (identified by staining with Kb-SIINFEKL multimers) were flow sorted from B6 mice immunized with either subunit vaccination (polyIC/aCD40) or inoculated with LM-OVA. using a FACSAria Fusion (BD Biosciences) and total RNA was Isolated using Qiagen RNeasy columns. (Figure 5A), the isolated RNA was reverse transcribed according to the vendors protocol (Invitrogen) and the resulting cDNA analyzed by gene array (Affymetrix MoGene-1_0-st-v1) according to the manufacturer's protocol. All genes differentially expressed genes (significant for adjusted P value, FDR<0.1) between vaccine and listeria responding T cells were identified using Transcriptome Analysis Console (TAC) Software (ThermoFisher). All genes associated with GO accession numbers 0008152 (metabolic process), 0006099 (tricarboxylic acid cycle), 0061621 (canonical glycolysis) as well as KEGG gene sets for oxidative phosphorylation, tricarboxylic acid cycle, and glycolysis were extracted and plotted for their fold change (greater than or equal to 1.1) against -log10 adjusted p-value.

RNAseq: Congenically marked WT or IL-$27R^{-/-}$ OT1 T cells were flow sorted 3 days after subunit vaccination using a FACSAria Fusion (BD Biosciences) and total RNA was isolated using Qiagen RNeasy columns. RNA was processed for next-generation sequencing (NGS) library construction as developed in the National Jewish Health (NJH) Genomics Facility for analysis with a HiSeq 2500 (Illumina). A SMARTer® Ultra™ Low Input RNA Kit for Sequencing – v4 (Clontech) and Nextera XT (Illumina) kit were used. Briefly, library construction started from isolation of total RNA species, followed by SMARTer 1st strand cDNA synthesis, full length dscDNA amplification by LD-PCR, followed by purification and validation. After that, the samples were taken to the Nextera XT protocol where the sample is simultaneously fragmented and tagged with adapters followed by a limited cycle PCR that adds indexes. Once validated, the libraries were sequenced as barcoded-pooled samples and run on the HiSeq 2500 by the NJH Genomics Facility. FASTQ files were generated using the Illumina bcl2fastq converter (version 2.17). Nextera TruSight adapters were trimmed with Skewer (version 0.2.2) (*67*), which by default removes reads with a remaining length of less than 18 nt. The quality of the reads was assessed using FastQC (version 0.11.5) (*68*) before and after read trimming. Trimmed reads were mapped with the STAR aligner (version 2.4.1d) (*69*) to the GRCm38 assembly of the mouse genome using gene using gene annotations from Ensembl version 84. Reads mapping to each gene of the Ensembl 84 annotation were counted with the featureCounts program from the Subread software package (v1.5.1) (*70*). The statistical comparison between WT and IL27Ra mutant samples was conducted using the Wald test in the DESeq2 package (version 1.14.1) (*71*) for the R statistical software (version 3.3.2) with a model correcting for sample batch effects. The p-values reported were adjusted for multiple testing using the method by Benjamini & Hochberg (*72*). The TPM counts for all genes associated with the GO metabolic pathways *metabolic process, tricarboxylic acid cycle*, and *electron transport chain* (GO:0008152, GO:0006099, and GO:0022900) were filtered to only include those with >1 tpm. The MetaboloAnalyst web-based resource (*73*) was used to identify all genes with a fold change >1.15 and significant for adjusted P value, FDR<0.1, and a heat map was generated through Morpheus (Broad Institute).

Proteomics analyses were performed via in solution tryptic digestion (Filter-Aided Sample Preparation method, as described (*74*) followed by nanoUHPLC-MS/MS (nano Easy LC II - Orbitrap Fusion Lumos, Thermo Fisher) on vaccine vs LM-OVA samples in triplicate.

Transmission Electron Microscopy

Sorted cells were fixed and pelleted in 2.5% glutaraldehyde and 2% paraformaldehyde in 0.1 M sodium cacodylate buffer (pH 7.4). The pellets were resuspended in 4% agarose that was allowed to harden and then cut into small pieces for processing. Cells were first rinsed three times in 0.1 M sodium cacodylate buffer, then post-fixed in 2% osmium tetroxide for 1 hour. After three washes in water, the cells were immersed in 2% uranyl acetate for 1 hour at 4^{o}C. The cells were again rinsed three times in water and then dehydrated through a graded ethanol series (25%, 50%, 75%, 90%, 95%, 100% x3) for 10 minutes each, and infiltrated with LX112 resin. The cells were embedded and cured for 48 hours at 60^{o}C in an oven. Ultra-thin sections (60 nm) were cut on a Reichert Ultracut S from a small trapezoid positioned over the cells and were picked up on copper mesh grids (EMS). Sections were imaged on a FEI Tecnai G2 transmission electron microscope with an AMT digital camera.

Supplementary Figures:

Figure S1

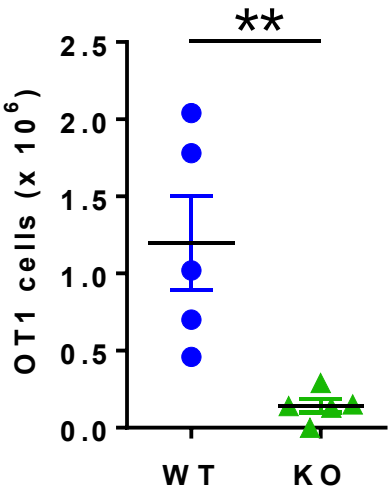

Figure S2

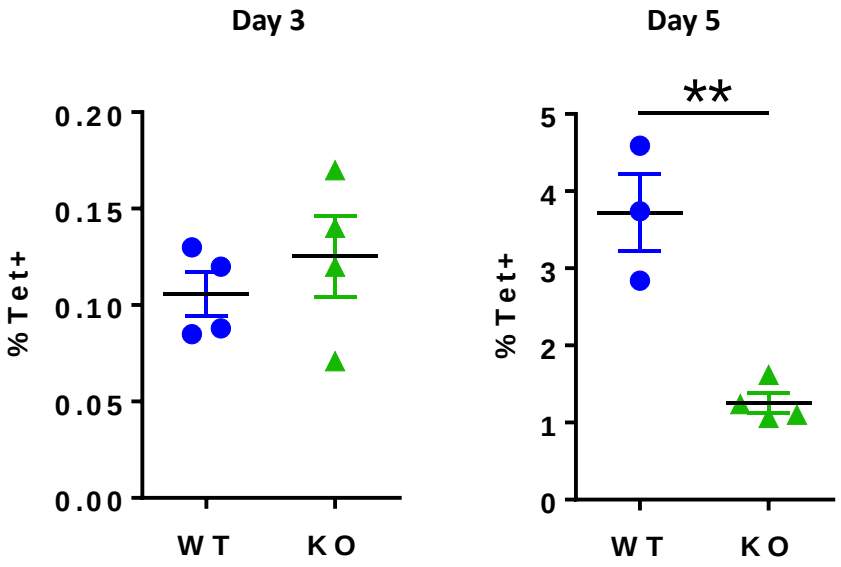

Figure S3

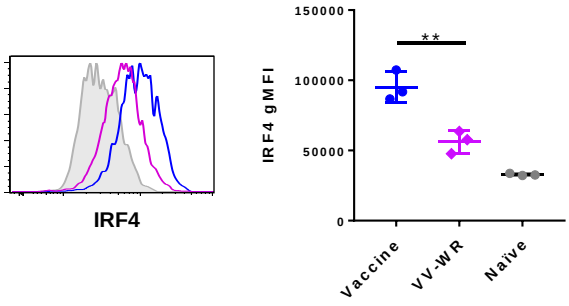

Figure S4

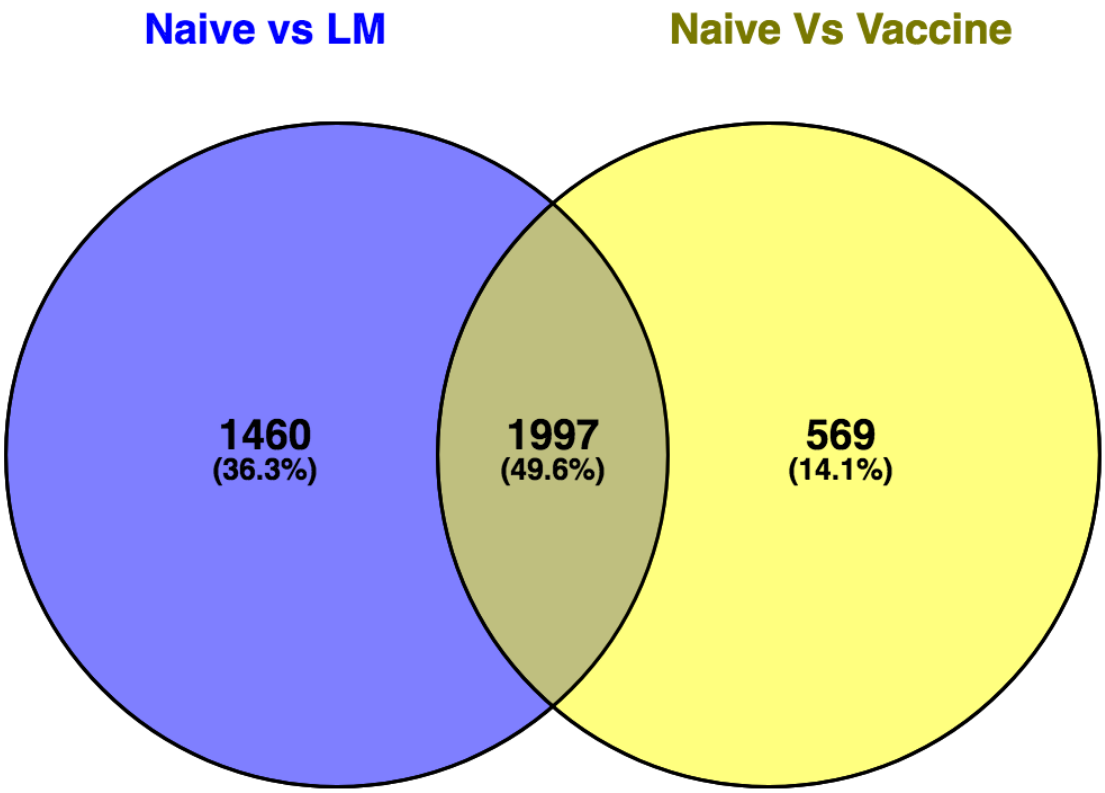

Figure S5

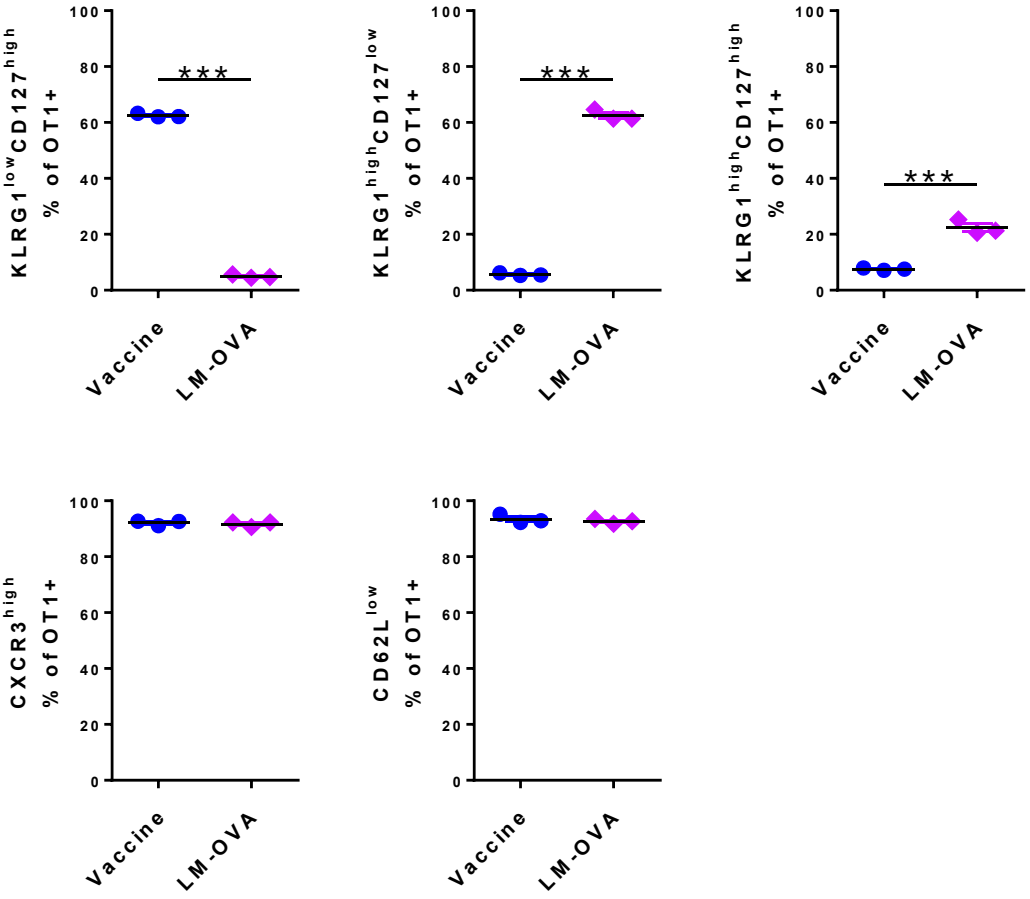
KLRG1low CD127high % of OT1+
KLRG1high CD127low % of OT1+
KLRG1high CD127high % of OT1+
CXCR3high % of OT1+
CD62Llow % of OT1+
***
Vaccine
LM-OVA
0
20
40
60
80
100

Figure S6

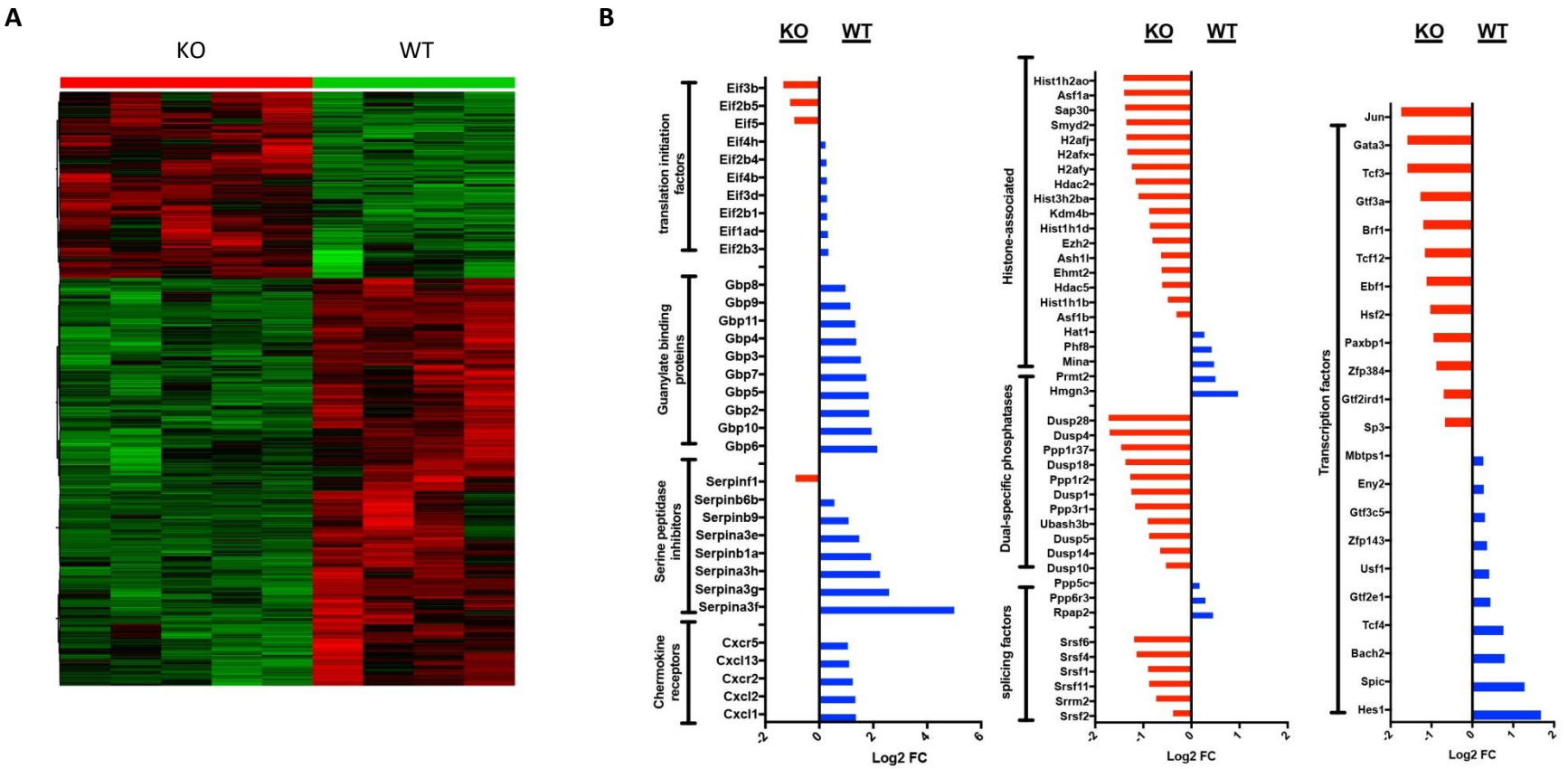
A
KO
WT
B
KO
WT
translation initiation factors
Eif3b
Eif2b5
Eif5
Eif4h
Eif2b4
Eif4b
Eif3d
Eif2b1
Eif1ad
Eif2b3
Guanylate binding proteins
Gbp8
Gbp9
Gbp11
Gbp4
Gbp3
Gbp7
Gbp5
Gbp2
Gbp10
Gbp6
Serine peptidase inhibitors
Serpinf1
Serpinb6b
Serpinb9
Serpina3e
Serpinb1a
Serpina3h
Serpina3g
Serpina3f
Chermokine receptors
Cxcr5
Cxcl13
Cxcr2
Cxcl2
Cxcl1
-2
0
2
4
6
Log2 FC
Histone-associated
Hist1h2ao
Asf1a
Sap30
Smyd2
H2afj
H2afx
H2afy
Hdac2
Hist3h2ba
Kdm4b
Hist1h1d
Ezh2
Ash1l
Ehmt2
Hdac5
Hist1h1b
Asf1b
Hat1
Phf8
Mina
Prmt2
Hmgn3
Dual-specific phosphatases
Dusp28
Dusp4
Ppp1r37
Dusp18
Ppp1r2
Dusp1
Ppp3r1
Ubash3b
Dusp5
Dusp14
Dusp10
splicing factors
Ppp5c
Ppp6r3
Rpap2
Srsf6
Srsf4
Srsf1
Srsf11
Srrm2
Srsf2
-2
-1
0
1
2
Log2 FC
Transcription factors
Jun
Gata3
Tcf3
Gtf3a
Brf1
Tcf12
Ebf1
Hsf2
Paxbp1
Zfp384
Gtf2ird1
Sp3
Mbtps1
Eny2
Gtf3c5
Zfp143
Usf1
Gtf2e1
Tcf4
Bach2
Spic
Hes1
-2
-1
0
1
2
Log2 FC

Figure S7

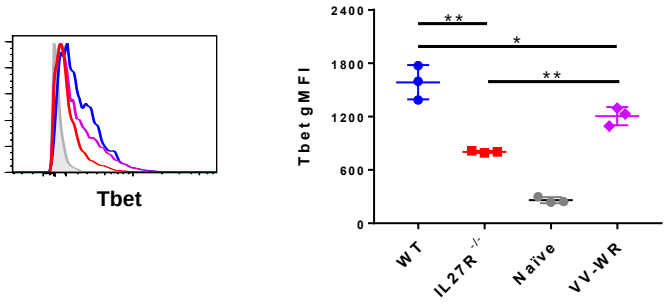

Supplemental figure legends.

Fig. S1. In response to subunit vaccination, the formation of T cell memory is substantially reduced in an IL-15$^{-/-}$ host.
One day prior to vaccination, 5,000 purified OT1 T cells were transferred I.V. into C57BL/6 or IL-15$^{-/-}$ recipients. Spleens were harvested 30 days after vaccination and the total number of OT1s were determined.

Fig. S2. IL-15 is required to support survival of vaccine-elicited T cells, not for their initial expansion to antigenic challenge.
The percentage of CD8 T cells that were tetramer positive in WT and IL-15$^{-/-}$ mice were analyzed at 3 and 5 days after vaccination.

Fig. S3. Vaccine-elicited T cells express levels of IRF4 substantially higher than in T cells responding to viral challenge.
IRF4 staining on tetramer-positive cells from vaccine and vaccinia virus 3 d.p.i.

Fig. S4. Vaccine- and infection-elicited T cells express both overlapping and unique gene sets when compared with naïve T cells.
Commonly and differentially upregulated genes, as compared to naïve T cells, in T cell responding to either vaccination or Listeria challenge. Gene expression in the indicated T cell subsets was analyzed by Affymetrix gene arrays as described in the materials and methods. Differentially expressed genes (significant for adjusted P value, FDR<0.1) were determined between naïve and vaccine (yellow circle) and naïve and listeria (blue circle) using Transcriptome Analysis Console (TAC) Software (ThermoFisher). These gene sets were then compared and the overlap represented in the Venn Diagram shown.

Fig. S5. Vaccine-elicited T cells express predominantly a central memory phenotype as compared with T cells responding to infection.
OT1 T cells were stained for KLRG1, CD127, CXCR3, and CD62L 5 d.p.i.

Fig. S6. Global gene expression differences and representative gene sets in WT versus IL-27R$^{-/-}$ T cells responding to subunit vaccination.
Differential gene expression between WT and IL-27R$^{-/-}$ T cells responding to vaccination. Gene expression in the WT and IL-27R$^{-/-}$ T cells was determined by RNAseq as described in the materials and methods 3 days after immunization. The statistical comparison between WT and IL27Ra mutant samples was conducted using the Wald test in the DESeq2 package (version 1.14.1) for the R statistical software (version 3.3.2) with a model correcting for sample batch effects. **A**. Individual sample TPMs were uploaded into the MetaboloAnalyst web-based resource and a heat map generated for all genes with a fold change >1.5 and significant for adjusted P value, FDR<0.1. **B**. Representative examples of some gene families regulated predominantly in WT (left graph), IL-27R-/- (middle graph), or both (right graph) are shown.

Fig. S7. Tbet expression in vaccine-elicited T cells from WT mice is elevated compared with WT T cells responding to virus infection.
Tbet staining on tetramer-positive cells from WT and IL-27R$^{-/-}$ mice 3 days after immunization or in WT mice 3 days after vaccinia virus infection.